Journal of Alloys and Compounds 509 (2011) 1424–1429

Contents lists available at ScienceDirect

Journal of Alloys and Compounds

journal homepage: www.elsevier.com/locate/jallcom

Magnetic characterization of polycrystalline $NdFeAsO_{0.88}F_{0.12}$ oxypnictide superconductor

Y. Ding[a], Y. Sun[a], X.D. Wang[a], Z.X. Shi[a,*], Z.A. Ren[b], J. Yang[b], W. Lu[b]

[a] *Department of Physics, Southeast University, Nanjing 211189, PR China*
[b] *Institute of Physics and Beijing National Laboratory for Condensed Matter Physics, Chinese Academy of Science, Beijing 100190, PR China*

ARTICLE INFO

Article history:
Received 24 August 2010
Received in revised form 3 November 2010
Accepted 5 November 2010
Available online 12 November 2010

PACS:
74.70.Xa
74.25.Ha
74.25.N–

Keywords:
High-T_c superconductors
Magnetization
Magnetic measurements
Granularity

ABSTRACT

The superconducting properties of polycrystalline $NdFeAsO_{0.88}F_{0.12}$ oxypnictide were studied by both DC and AC magnetization measurements. The zero-field cooled (ZFC) magnetic susceptibility, $\chi(T)$, measured under the magnetic field of 0.5 T shows a dramatic decrease at about 11 K. The imaginary component of the first harmonics of the AC magnetic susceptibility, $\chi''(T)$, increases with the increasing DC field H_{dc} below 11 K. These results indicate the onset of robust intergranular superconductivity at low temperatures. The magnetic hysteresis loops show an anomalous double central peak effect at low temperatures, with one peak at positive fields in decreasing positive external fields. This phenomenon suggests the granular character of this system. The paramagnetism of Nd^{3+} ions tilts the magnetic hysteresis loops and broadens the hysteresis width ΔM. After correction for the paramagnetism, the temperature and field dependence of the average magnetization critical current density J_{cm} was obtained. The related mechanism was discussed.

1. Introduction

The recent discovery of superconductivity at 26 K in the iron oxypnictide LaFeAs(O, F) [1] has stimulated great interests among condensed-matter physics community. Tremendous work was carried out, leading to the emergence of novel iron-based superconductor families with different crystal structures: 1 1 1 1 (REFeAs(O, F)), 1 2 2 ((Ba, K)Fe_2As_2) [2], 1 1 1 (LiFeAs) [3] and 1 1 (Fe(Se, Te)) [4]. The REFeAs(O, F) superconductors, in which T_c is over 50 K when La is replaced by Sm [5], Gd [6] or Tb [7], crystallize in the tetragonal $P4/nmm$ space group with two formula units per unit cell. The crystal structure consists of alternating RE–O and Fe–As layers stacked along the c axis. Since magnetic elements such as Fe and rare earths exist in this system, relevant questions have been raised about the relationship between magnetism and superconductivity. Muon spin rotation (μSR), neutron, and Mossbauer measurements [8,9] on undoped LaFeAsO have revealed commensurate spin density wave (SDW) ordering of the Fe moments below $T_N = 135$ K with amplitude of $0.35\mu_B$. Superconductivity can be induced from the magnetically ordered parent compound by carrier doping or external or internal pressure. Some measurements suggest that the magnetic order is rapidly suppressed upon doping and the maximum T_c is achieved just as static magnetism disappears [8,10]. Tarantini et al. excluded the long-range antiferromagnetic order in the superconducting $NdFeAsO_{0.94}F_{0.06}$ [11], consistent with neutron measurements down to 1.5 K [12]. However, μSR results suggest that long range magnetic ordering may exist below 2.4 K for Nd-1 1 1 1 and below 4 K for Ce-1 1 1 1 compounds [13]. Drew et al. detected magnetic fluctuations [14] and static magnetism [15] coexisting in the $SmFeAsO_{1-x}F_x$ by μSR, and Ryan et al. detected the coexistence of long-ranged magnetic order and superconductivity in $SmFeAsO_{1-x}F_x$ by using neutron diffraction [16]. The coexistence of magnetism and superconductivity, and the role played by magnetism in the basic superconducting mechanism need to be further investigated both theoretically and experimentally.

Besides the studies related to the superconducting mechanism, it is also necessary to study the vortex pinning properties, which are of great importance on potential applications. Recent reports have shown the modified electromagnetic behavior [11,17,18] by magnetism of rare earth ions and the granularity [19–21] in the 1 1 1 1 system. Our previous work [22] shows that weak links and strong links coexist in the Nd-1 1 1 1 system, and the strong links persist up to 9 T. In this paper, both DC and AC magnetization measurements were performed to study the vortex pinning properties of the $NdFeAsO_{0.88}F_{0.12}$ superconductor. The influence of

---

* Corresponding author.
E-mail address: zxshi@seu.edu.cn (Z.X. Shi).

0925-8388/$ – see front matter © 2010 Elsevier B.V. All rights reserved.
doi:10.1016/j.jallcom.2010.11.050

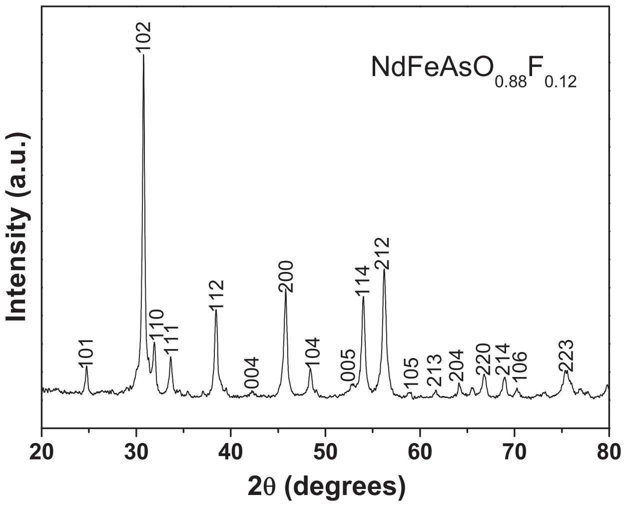

Fig. 1. X-ray powder diffraction patterns of the $NdFeAsO_{0.88}F_{0.12}$ sample.

paramagnetism of Nd^{3+} ions on the magnetization critical current density was also investigated.

2. Experimental

The polycrystalline $NdFeAsO_{1-x}F_x$ superconducting sample was prepared directly by a high-pressure method similar to [23]. The starting materials were mixed according to the nominal stoichiometric ratio of $NdFeAsO_{0.88}F_{0.12}$, then ground thoroughly and pressed into pellets. The pellets were sealed in boron nitride crucibles and sintered under 6 GPa in a high-pressure synthesis apparatus at the temperature of 1250 °C for 2 h. The sample had the dimensions of 1.16 mm × 1.88 mm × 4.50 mm, a mass of 58 mg and is therefore about 82% of the theoretical density (7.21 g/cm^3).

The crystal structure of the sample was characterized by powder X-ray diffraction (XRD) on an MXP18A-HF–type diffractometer with Cu-Kα radiation from $2\Theta = 20–80°$ with a step-scan of 0.01 °. As shown in Fig. 1, all main peaks can be well indexed based on the ZrCuSiAs tetragonal structure, confirming the formation of NdFeAs(O, F) phase. No impurity peak was observed.

DC magnetization $M(T)$ and $M(H)$ measurements were performed using a vibrating sample magnetometer (VSM) of a Quantum Design PPMS. Magnetic critical current densities J_{cm} were estimated using the Bean model from the $M(H)$ hysteresis loops (MHLs). By using the PPMS equipped with an AC susceptometer, the first harmonics of the AC magnetic susceptibility as a function of the temperature were measured at various frequencies, ν, AC magnetic field amplitudes, h_{ac}, and DC fields, H_{dc}, which were parallel to the AC field. Before each measurement, the magnetic field was oscillated to reduce the residual field and the sample was warmed up to 60 K to fully expel the flux trapped inside. Sufficient waiting time was adopted to ensure the thermal homogeneity. During both DC and AC measurements, the magnetic fields were applied along the longest dimension of the sample.

3. Results and discussion

3.1. The DC magnetic susceptibilities

The DC magnetic susceptibilities $\chi(T)$ were measured by zero-field cooling (ZFC) and field cooling (FC) under 1.5 mT and 0.5 T. Fig. 2(a) shows the $\chi(T)$ curves measured under 1.5 mT. The sharp diamagnetic superconducting transition indicates good sample quality. After demagnetization correction, the superconducting shielding volume fraction was estimated to be 78%, confirming bulk superconductivity. The transition temperature T_c determined by the onset of diamagnetic signal is about 50 K. Fig. 2(b) shows the $\chi(T)$ curves measured under 0.5 T. The magnetic fields suppressed the superconducting diamagnetism, and most part of the ZFC curve became positive due to the strong paramagnetic background. It is also noted that the ZFC curve shows a sharp decrease and a broad shoulder at about 11 K. Similar behavior was reported by several groups in Nd [11], Sm [18] and Pr [24] 1111 superconductors. To investigate the origin of this behavior, the paramagnetic background was evaluated and subtracted from the total susceptibilities. Assuming that the paramagnetic magnetic moments of the Nd^{3+} ions do not interact with each other, the paramagnetic magnetization is expected to be given by

$$M_{\mathrm{pm}} = M_0 B_{\mathrm{J}}\left(\frac{g\mu_{\mathrm{B}}JB}{k_{\mathrm{B}}(T+\Theta)}\right) \qquad (1)$$

where g is the Lande factor, μ_B is the Bohr magneton, k_B is the Boltzmann constant, $B_J(x)$ is the Brillouin function and $M_0 = NgJ\mu_B$, N is the number of Nd ions per unit volume. A phenomenological parameters Θ was introduced because the electric crystal field (CEF) acting on Nd 4f electrons splits and mixes the degenerated $|JM_J\rangle$ states resulting in, for $g\mu_B JB/k_B T \ll 1$, the modification of the Curie form $\chi = C/T$ to the Curie–Weiss law, $\chi = C/(T+\Theta)$ [25]. According to the Russell–Saunders coupling model the ground state term of the Nd^{3+} ion is $^4I_{9/2}$ ($J = 9/2$).

The $M(T)$ curve measured from 50 to 300 K under 0.75 T was plotted in Fig. 2(c), showing the Curie–Weiss behavior similar to reference [26]. The paramagnetic background of total magnetization from 5 to 50 K was obtained by fitting the measured $M(T)$ curve using Eq. (1) with parameter $\Theta = 16$ K and $M_0V = 3.26 \times 10^{-3}$ A m^2, where V is the sample volume. The density of Nd^{3+} ions as obtained is 1.22×10^{28} m^{-3}, agreed with the actual value of 1.09×10^{28} m^{-3}. The 0.5 T paramagnetic background-subtracted $\chi(T)$ curves are presented in Fig. 2(d). The $\chi(T)$ curves show negative values below the superconducting onset temperature, indicating the diamagnetic effect. The shoulder in the ZFC $\chi(T)$ curve disappeared. The FC $\chi(T)$ curve in Fig. 2(d) increases below 15 K. This may be caused by the underestimating of the paramagnetic component at low temperature, where the M_{pm} value deviates from Eq. (1). The dramatic decrease on ZFC 0.5 T $\chi(T)$ curve at about 11 K is not likely caused by small amounts of magnetic impurities, which were not detected by XRD analysis. The possible impurities in Nd-1 1 1 1 sample are Nd_2O_3, NdOF, Fe_2O_3, FeF_2, Fe–As and Nd–Fe systems. Nd_2O_3 and NdOF are paramagnetic at low temperatures [11,27], small amounts of antiferromagnetic FeF_2, Fe_2As, FeAs and $FeAs_2$ with T_N of 78 [28,29], 353, 77 and <5 K [30], respectively, should not have decisive effect on $M(T)$ behavior from 5 to 50 K. The existence of ferromagnetic Fe_2O_3 and Nd–Fe systems with Curie temperatures of more than 273 K [31] can be excluded by $M(H)$ measurements presented later. In a previous report [24], the decrease in $\chi(T)$ was explained by the onset of intergranular superconductivity. AC magnetic susceptibilities measurements were performed to further investigate this system, since the onset of superconductivity will cause a peak in the imaginary part of the χ'', representing losses due to field penetration.

3.2. The AC magnetic susceptibilities

Fig. 3(a) shows the AC magnetic susceptibilities χ' and χ'' as function of temperature at frequencies of 100 Hz, 500 Hz and 1 kHz, for DC magnetic fields $\mu_0 H_{dc} = 0.5$ T and the AC magnetic field $\mu_0 h_{ac} = 0.8$ mT. As the frequency decreases, the transition temperature shifts to lower values and the peak height in χ'' decreases as it moves to lower temperatures. Fig. 3(b) shows the $\chi'(T)$ and $\chi''(T)$ curves measured at the fixed frequency $\nu = 500$ Hz, $\mu_0 h_{ac} = 1.6$ mT and at various $\mu_0 H_{dc} = 5$ mT, 15 mT, 50 mT, 0.5 T and 0.75 T. As the DC fields increase, the transition in $\chi'(T)$ and $\chi''(T)$ becomes broad and the peak height in χ'' decreases as it moves to lower temperature. These features are similar to that of high-temperature superconductors [32,33] and can be explained by flux creep and the temperature dependence of shielding currents [34]. It is noted that in Fig. 3(a), χ'' increased at low temperatures, and in Fig. 3(b), a weak peak in χ'' at about 11 K emerges when $\mu_0 H_{dc} = 50$ mT and the peak seems to move below 5 K when $\mu_0 H_{dc}$ reaches 0.5 T. These features may be explained by the onset of intergranular